On cold spells in North America and storminess in western Europe

Gabriele Messori, Rodrigo Caballero, Marco Gaetani

▶ **To cite this version:**

Gabriele Messori, Rodrigo Caballero, Marco Gaetani. On cold spells in North America and storminess in western Europe. Geophysical Research Letters, 2016, 43 (12), pp.6620-6628. 10.1002/2016GL069392 . insu-01327494

HAL Id: insu-01327494
https://insu.hal.science/insu-01327494

Submitted on 19 Jul 2020

HAL is a multi-disciplinary open access archive for the deposit and dissemination of scientific research documents, whether they are published or not. The documents may come from teaching and research institutions in France or abroad, or from public or private research centers.

L'archive ouverte pluridisciplinaire **HAL**, est destinée au dépôt et à la diffusion de documents scientifiques de niveau recherche, publiés ou non, émanant des établissements d'enseignement et de recherche français ou étrangers, des laboratoires publics ou privés.

AGU PUBLICATIONS

Geophysical Research Letters

RESEARCH LETTER
10.1002/2016GL069392

Key Points:
- Cold spells over the eastern USA correspond to a very zonal and intense jet
- Cold spells over the eastern USA match statistically heightened surface wind destructiveness and precipitation over western Europe
- The cold spells are preceded by a negative NAO and followed by a positive PNA

Supporting Information:
- Supporting Information S1

Correspondence to:
G. Messori,
gabriele.messori@metoffice.gov.uk

Citation:
Messori, G., R. Caballero, and M. Gaetani (2016), On cold spells in North America and storminess in western Europe, *Geophys. Res. Lett.*, *43*, 6620–6628, doi:10.1002/2016GL069392.

Received 16 DEC 2015
Accepted 2 JUN 2016
Accepted article online 4 JUN 2016
Published online 24 JUN 2016

©2016. American Geophysical Union. All Rights Reserved.

On cold spells in North America and storminess in western Europe

Gabriele Messori[1,2], Rodrigo Caballero[1], and Marco Gaetani[3]

[1]Department of Meteorology and Bolin Centre for Climate Research, Stockholm University, Stockholm, Sweden, [2]Now at Met Office Hadley Centre, Exeter, UK, [3]LATMOS/IPSL, UPMC Université Paris 06 Sorbonne Universités, UVSQ, CNRS, Paris, France

Abstract We discuss the dynamical and statistical links between cold extremes over eastern North America and storminess over western Europe, with a focus on the midlatitude jet stream, the North Atlantic Oscillation (NAO) and the Pacific-North American Pattern (PNA). The analysis is performed on the European Centre for Medium-Range Weather Forecasts 20th Century Reanalysis. The large-scale circulation associated with the cold spells corresponds to advection of cold air from the Arctic region into North America and to a very zonal and intense North Atlantic jet, shifted persistently south of its climatological location. These features of the Atlantic jet are conducive to destructive windstorms and intense precipitation over a large part of southern and continental Europe and the British Isles. The cold spells are preceded by a negative NAO and followed by a positive PNA; however, we interpret the associated circulation anomalies as being distinct from these standard modes of climate variability.

1. Introduction

A remarkably large number of extreme weather events have affected the extratropical Northern Hemisphere during recent winters [e.g., *Coumou and Rahmstorf*, 2012; *Screen and Simmonds*, 2014; *Francis and Skific*, 2015]. Repeated cold and snowy spells over North America [e.g., *Wang et al.*, 2010; *Guirguis et al.*, 2011; *Palmer*, 2014; *Lee et al.*, 2015; *Trenary et al.*, 2015] and stormy and rainy weather over continental Europe and the British Isles [e.g., *Fink et al.*, 2009; *Matthews et al.*, 2014; *Huntingford et al.*, 2014; *Slingo et al.*, 2014; *Kendon and McCarthy*, 2015; *van Oldenborgh et al.*, 2015; *Christidis and Stott*, 2015; *Wild et al.*, 2015] have garnered widespread scientific and media coverage. Detailed case studies have been dedicated to individual events [e.g., *Fink et al.*, 2009; *Wang et al.*, 2010] and seasons [e.g., *Santos et al.*, 2013; *Huntingford et al.*, 2014; *Kendon and McCarthy*, 2015], while other studies have focused more broadly on the drivers of cold spells over North America and storminess over Europe. The occurrence of these events has notably been ascribed to large-scale modes of variability [e.g., *Wang et al.*, 2010; *Guirguis et al.*, 2011; *Huntingford et al.*, 2014] and changes in midlatitude planetary wave activity [e.g., *Liu et al.*, 2012; *Barnes and Screen*, 2015].

Cold extremes over North America and storminess over Europe have typically been discussed separately. However, the notable recent co-occurrence of the two types of extremes in the same winter [*Kendon and McCarthy*, 2015; *Trenary et al.*, 2015] raises the question of whether there may be a systematic, physically based link between the two. The answer to this question can have important consequences for insurance and reinsurance companies with worldwide exposure that are particularly vulnerable to large, correlated losses across their portfolios. An analogous situation arises for "clustered" windstorms, where specific dynamical mechanisms favor the occurrence of several extreme windstorms in quick succession [*Pinto et al.*, 2014].

Here we explore the dynamical links between extreme events across the North Atlantic basin. We specifically seek to identify systematic connections between cold spells over eastern North America and downstream impacts over western Europe, in particular intense surface wind and precipitation events. North American cold spells are defined here on time scales of days, since monthly or longer-term temperature means can be misleading and conceal severe, short-lived events [e.g., *Gu et al.*, 2008]. We find that the large-scale flow patterns typically associated with severe cold spells are likely distinct from climate modes of variability, such as the North Atlantic Oscillation (NAO) and the Pacific-North American Pattern (PNA), since they are comparatively rare [*Grotjahn et al.*, 2015]. This does not exclude climate modes from providing favorable conditions for the generation of these patterns and the associated extreme events [*Loikith and Broccoli*, 2014], and we discuss them in this context.

We begin by defining an objective index of cold spells over eastern North America (section 2). An analysis of the composite anomalies in various atmospheric variables confirms that our set of cold spells presents a

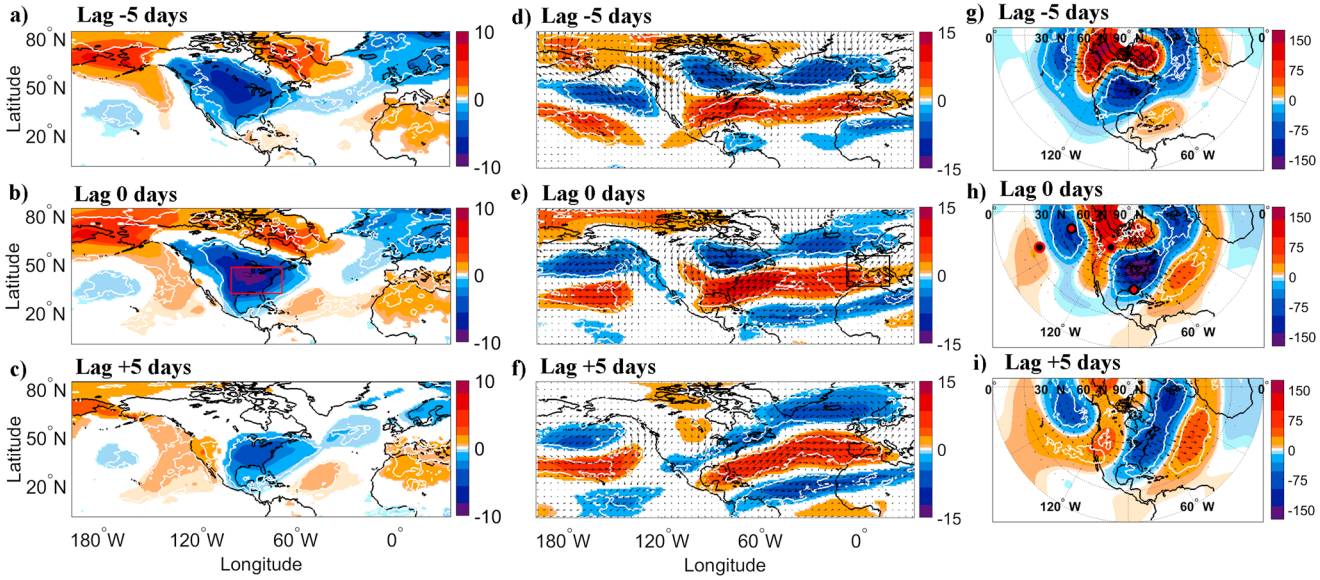

Figure 1. Surface temperature anomalies (K) during North American cold spells at lags of (a) −5, (b) 0, and (c) +5 days. The 250 hPa wind anomalies (arrows) and 250 hPa wind speed anomalies (m s^{-1}, shading) during North American cold spells at lags of (d) −5, (e) 0, and (f) +5 days. The red box in Figure 1b marks the domain over which the cold spells are selected; the black box in Figure 1e marks the domain over which the PDI and rainfall anomaly are computed. Horizontal wave activity flux (arrows) and 250 hPa geopotential height anomalies (m, shading) during North American cold spells at lags of (g) −5, (h) 0, and (i) +5 days. The dots in Figure 1h mark the locations used to compute the PNAI. Only anomalies exceeding the 95% confidence level derived from a random Monte Carlo sampling procedure are shown in Figures 1a–1f. All values are displayed in Figures 1g–1i to highlight the wave-like pattern of the geopotential height anomalies. The white contours in all panels mark areas where at least two thirds of the events agree on the sign of the anomalies. The data covers ERA-20C DJFs over the period 1900–2010.

qualitatively homogeneous dynamical evolution, which results in common large-scale flow anomalies over the Atlantic and associated weather extremes over a large part of western Europe (section 3). This development is then related to climate modes of variability that have previously been associated with cold spells over North America (section 4). Finally, section 5 contextualizes and summarizes our findings.

2. Climatology of North American Cold Spells

We use the European Centre for Medium-Range Weather Forecasts 20th Century Reanalysis product (ERA-20C) [*Poli et al.*, 2016]. Daily mean fields at 1° horizontal resolution are considered. The analysis spans 111 winters (December–February (DJF)), from January 1900 to December 2010. Statistical significance is assessed using both a Monte Carlo approach with 1000 random samples and a sign test showing areas where at least two thirds of the composited events agree on the sign of the anomalies. Furthermore, the standard deviations of the composite surface temperature and wind speed anomalies discussed in sections 2–5 are shown in Figure S1 in the supporting information.

Cold spells in North America are defined over a domain in the eastern portion of the continent (30°N–45°N, 100°W–70°W; red box in Figure 1b), selected to resemble domains previously used in the literature [*Walsh et al.*, 2001]. The sensitivity to the exact choice of domain is discussed in Text S2 in the supporting information. Two-meter air temperature anomalies are computed as deviations from the daily climatology and are then smoothed with a 7 day running mean, following *Yu et al.* [2015a]. The events are ranked based on the area-weighted, domain-averaged anomaly; any days within 3 weeks of a colder day are eliminated. So, for example, if the four coldest events in our time series were days 10, 71, 60, and 15, only days 10 and 71 would be retained. This separation was selected based on the long persistence of the circulation anomalies associated with the cold spells (see section 3). The top 60 events are then retained for analysis. All lags are relative to the day of peak negative temperature anomalies. Most of the analysis presented in sections 3–5 was repeated on the 20 coldest spells identified in the ERA-Interim data [*Dee et al.*, 2011] over the period January 1979 to December 2011, and the main conclusions we draw were found to be qualitatively robust (not shown).

Figures 1a–1c display composite temperature anomalies for the selected cold spells at lags of −5 to +5 days. In agreement with previous analyses, the cold anomalies are first evident over central and eastern Canada and successively extend to the lower latitudes over several days [e.g., *Walsh et al.*, 2001; *Portis et al.*, 2006].

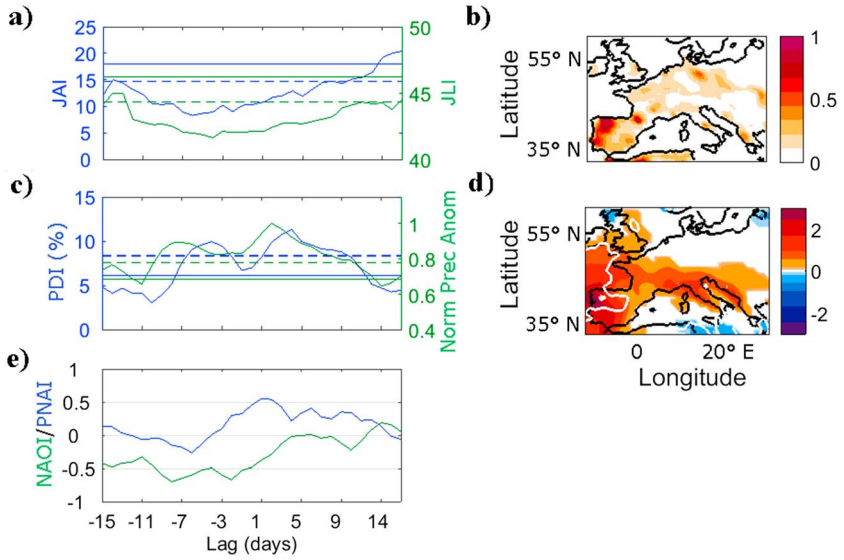

Figure 2. (a) JAI (200–400 hPa, blue) and JLI (200–400 hPa, green). (b) Composite PD values over lags −5 to +5 days, normalized to the interval (0, 1). (c) PDI (blue) and rainfall anomaly (green). (d) Mean composite precipitation anomalies (mm d^{-1}) over lags −5 to +5 days; only anomalies exceeding the 95% confidence level derived from a random Monte Carlo sampling procedure are shown. (e) PNAI (blue) and NAOI (green) values at multiple time lags. All values and lags refer to the North American cold spells. The continuous horizontal lines in Figures 2a and 2c mark the wintertime average values. The dashed horizontal lines mark the (a) 5th and (b) 95th percentiles, derived from a random Monte Carlo sampling procedure. The rainfall anomalies in Figure 2c are area-weighted values cumulated over all gridboxes in the domain, summed over 3 day periods and normalized to have a maximum value of +1. The abscissa in Figure 2c indicate the central days of the 3 day intervals. The white contours in Figure 2d mark areas where at least two thirds of the events agree on the sign of the anomalies. The data covers the same range as Figure 1.

At the same time, warm anomalies appear over the Bering Strait region and the Labrador Sea. The full temporal evolution of the cold spells is shown in Figure S4. We note that a weak negative temperature anomaly is already present over central Canada 2 weeks before the peak of the cold spell. The area-weighted mean temperature anomaly value over the selection domain at lag 0 is −10.7°C for the coldest spell, −6.1°C for the warmest cold spell, and −7.7°C for the 60-event average.

3. Dynamical Evolution of North American Cold Spells and Impacts Over Europe

Cold spells in eastern North America are characterized by a circulation anomaly pattern featuring a large-scale, quasi-stationary cyclone over the Great Lakes and a dipole in the Pacific sector with anticyclonic circulation around the Bering Strait and a cyclone to the south (Figures 1d and 1e and 1g and 1h). All anomalies are computed following the same methodology as for 2 m temperature (see section 2). As for the temperature anomalies, these large-scale features start forming up to 2 weeks before the peak of the cold spell, intensify as the event progresses and then weaken after the peak (Figures 1f and S5). The maximum strength of the 250 hPa geopotential height anomaly pattern is seen a few days before the peak of the cold spell, with local anomalies in excess of 180 m (Figures 1g–1i). Figures 1g–1i also display the wave activity flux associated with these anomalies, computed following *Takaya and Nakamura* [2001]. Its relevance to the evolution of the cold spells is discussed in section 5. The concurrent upper level wind anomalies are consistent with the north-westerly advection of cold polar air toward the eastern United States (Figures 1d and 1e), which is a robust characteristic of cold spells in the region [e.g., *Konrad and Colucci*, 1989; *Walsh et al.*, 2001; *Loikith and Broccoli*, 2012].

Significant flow anomalies in the days preceding the North American temperature minima are also seen over the Atlantic sector, with a strong anticyclone over Greenland and a cyclonic anomaly further south (Figures 1g–1i). This pattern projects onto the negative phase of the NAO (see section 4) and yields a very southward-displaced, zonally oriented and intense Atlantic jet (Figures 1d–1f). The positive anomalies in the westerly flow extend across the Atlantic basin into Southwestern Europe. The anomalies in the jet entry region peak around day 0, while those over the eastern part of the basin, retain an approximately constant magnitude at positive lags. To provide an objective assessment of this behavior we apply the Jet Angle Index (JAI) of *Messori and Caballero* [2015]

Table 1. Jet Angle and Jet Latitude Values Over the North Atlantic and Potential Destructiveness Values Over Western Europe for the Wintertime Climatology and Different Subsets of Winter Days[a,b]

Events	Pressure Levels	Angle	Latitude	Peak PDI
(i) Wint. Clim.	700–925 hPa	(18.6)	(46.7)	
	200–400 hPa	(18.0)	(46.2)	
(ii) Eastern	700–925 hPa	10.8	42.1	11.3%
	200–400 hPa	8.9	41.6	
(iii) NAO+	700–925 hPa	20.8	49.2	9.5%
	200–400 hPa	21.8	48.8	
(iv) NAO−	700–925 hPa	9.3	41.2	4.7%
	200–400 hPa	6.0	40.8	
(v) PNA+	700–925 hPa	(18.8)	46.4	(5.8%)
	200–400 hPa	(18.2)	45.6	
(vi) PNA−	700–925 hPa	(18.2)	(46.6)	(5.6%)
	200–400 hPa	(18.1)	(46.2)	

[a] Jet Angle Index and Jet Latitude Index values at upper and lower levels for (i) the DJF climatology, (ii) eastern cold spells lag −4 days, (iii) positive and (iv) negative NAO phases (defined as NAOI > 1 and NAOI < −1, respectively), and (v) positive and (vi) negative PNA phases (defined as PNAI > 1 and PNAI < −1, respectively).

[b] The last column displays the peak PDI value over lags −5 to +5 days from the reference event. To ensure well-separated events, only cases where the NAOI and PNAI exceed the relevant threshold for more than 1 day are retained. The reference event is then the peak NAOI or PNAI value. The values in brackets are not statistically different from the wintertime climatology at the 95% confidence level.

and a Jet Latitude Index (JLI) similar to that first proposed by *Woollings et al.* [2010a]. The JAI quantifies the tilt of the jet, providing a bearing relative to due east for each time step; the JLI quantifies its meridional location, providing a latitude matching the strongest zonal flow across the basin; full details of both algorithms are provided in Texts S4 and S5. The cold spells are associated with anomalously low JLI and JAI values, in both the days preceding and immediately following the peak negative temperature anomalies (Figure 2a and Table 1).

Previous studies have found that an unusually strong jet can act to intensify Atlantic weather systems [*Rivière and Joly*, 2006; *Gómara et al.*, 2014a], while the enhanced zonality steers them toward Europe, favoring destructive winds over a region encompassing France, Germany, and Benelux [*Hanley and Caballero*, 2012; *Messori and Caballero*, 2015]. A similar pattern, with large anomalies in both the jet's bearing and intensity, is also associated with surface wind extremes over the western Mediterranean [*Raveh-Rubin and Wernli*, 2015]. We quantify surface wind destructiveness by adopting an empirical expression, motivated by considerations of surface power dissipation [*Klawa and Ulbrich*, 2003]. The potential destructiveness (PD) at a given grid point for a specific time-step is defined as

$$\mathrm{PD} = \begin{cases} ({}^{v}/_{v_{98}} - 1)^3, & v > v_{98} \\ 0, & v < v_{98} \end{cases} \quad (1)$$

Here v is the peak daily 10 m wind speed based on 3-hourly data at the chosen grid point and v_{98} is the climatological 98th percentile of v at the same location. By definition, the wind destructiveness is therefore nonzero on less than 2 days per winter on average. Figure 2b displays the composite PD values associated with the cold spells, summed over lags −5 to +5 days and normalized to the interval (0, 1). These lags roughly match the days over which the jet displays both the strongest intensification and significantly negative JLI and JAI anomalies (Figures 1, 2a, and S5). High PD values can be seen extending across western Europe and the Mediterranean region, with scattered areas of destructiveness extending into eastern Europe. To illustrate the temporal evolution of the PD over western Europe and the Mediterranean, we define the PD index (PDI) as the cumulative fraction of land gridboxes within the domain (35°N–52.5°N, 10°W–15°E; black box in Figure 1e) experiencing a nonzero PD over a consecutive 3 day period. This is designed to isolate spatially and temporally extensive destructive events as opposed to intense but isolated occurrences. The domain is chosen based on Figure 2b to encompass the areas displaying large PD values. The climatological PDI wintertime domain-mean value is 6.6%. Statistically significant increases in destructiveness rates are found at both positive and negative lags; the peak composite PDI value exceeds 11% (Figure 2c). We note that this value is well in excess of that associated with the positive NAO (Table 1), which is often linked to enhanced storminess over the Atlantic [e.g., *Gómara et al.*, 2014b]. The origin of the double peak in the PDI index is discussed in detail in Text S6. Of the 60 cold spells analyzed here, 48 display at least one PDI value above the wintertime mean over the lags −5 to +5 days, exceeding the 5% significance level obtained from random sampling.

Along with increased destructiveness, there are also positive precipitation anomalies across a large part of the domain, albeit with a low sign confidence (Figure 2d). These persist over several days and roughly match the

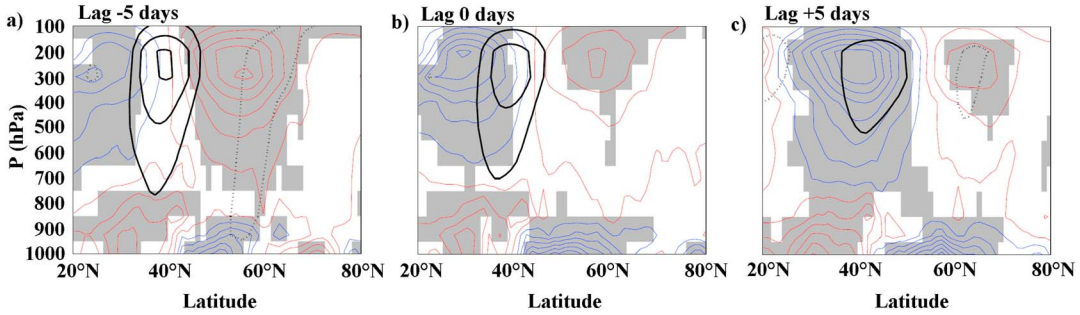

Figure 3. Anomalies of zonal wind (solid and dotted black contours, for positive and negative anomalies respectively, interval 2 m s^{-1}) and ageostrophic meridional wind (red and blue contours, for positive and negative anomalies respectively, interval 0.2 m s^{-1}), averaged over the range 10°W–5°E during North American cold spells at lags of (a) −5, (b) 0, and (c) +5 days. The grey shadings mark the anomalies in ageostrophic meridional wind exceeding the 95% confidence level derived from a random Monte Carlo sampling procedure. The data covers the same range as Figure 1.

period of enhanced destructiveness (Figure 2c). It has been shown that the interaction between the exit region of the midlatitude jet and the entry region of the subtropical jet affects the rainfall distribution over Europe, through the ageostrophic cross-jet circulation which modulates the vertical motions favorable to convection and precipitation [*Gaetani et al.*, 2011]. The evolution of the jet and cross-jet ageostrophic circulation over western Europe is presented in Figure 3 through the anomalies of the zonal and ageostrophic meridional wind, averaged over the range 10°W–5°E. This is chosen to match the most intense and geographically extensive precipitation anomalies shown in Figure 2d; however, the results we present are largely insensitive to small zonal shifts in the selected domain (see Figure S7). The ageostrophic wind meridional component, v_a, is computed as

$$v_a = v - v_g = v - \frac{1}{f}\frac{\partial \phi}{\partial x} \tag{2}$$

Here v is the meridional wind and φ is the geopotential height. A sizable jet anomaly around 40°N from day −5 to day 0 is accompanied by a v_a convergence (divergence) anomaly in the lower (upper) troposphere around 40–45°N. This indicates favorable conditions for vertical velocity anomalies, in turn leading to instability and positive precipitation anomalies. Day +5 is characterized by a weakening of the jet anomaly and a small northward shift of the associated ageostrophic meridional circulation to around 50°N. The enhanced zonality of the circulation also corresponds to a positive temperature anomaly across most of the Mediterranean basin (Figures 1a–1c), in agreement with previous analyses [e.g., *Kutiel et al.*, 1996; *Maheras et al.*, 1999].

The significant positive PDI and precipitation anomalies correspond to significant negative JAI and JLI anomalies (cf. Figures 2a and 2c), suggesting that the increased storminess and precipitation are directly related to the anomalously zonal and southern jet. This is confirmed by analyzing an objectively selected set of days with such jet characteristics (see Text S8).

4. Relation With Large-Scale Modes of Variability

Cold temperatures over North America and storms affecting Europe are often discussed in the context of the Pacific-North American Pattern (PNA) and the NAO [e.g., *Leathers et al.*, 1991; *Gómara et al.*, 2014b]. Here we investigate whether the large-scale patterns and anomaly fields discussed in section 3 are the direct results of strong projections on either of these variability patterns.

We compute the PNA index (PNAI) by combining the standardized 500 hPa geopotential height anomalies at 20°N, 160°W; 45°N, 165°W; 55°N, 115°W; and 30°N, 85°W (marked by the dots in Figure 1h), following *Wallace and Gutzler* [1981] and *Cellitti et al.* [2006]. The daily NAO index (NAOI) is similarly defined as the normalized difference between the standardized sea level pressure anomalies at 39°N, 9°W and 64°N, 22°W. Positive and negative modes are defined as NAOI, PNAI > 1 and NAOI, PNAI < -1, respectively.

As shown in Figure 2e, the NAO shifts from a significantly negative to a neutral phase as the cold spells evolve, in agreement with previous work [*Walsh et al.*, 2001; *Cellitti et al.*, 2006; *Yu et al.*, 2015b]. The negative NAO phase is

typically associated with below-average JAI and JLI values (Table 1), and indeed, the low NAOI values prior to the peak of the cold spells match the maximum zonalization and southward shift of the jet stream (cf. Figures 2a and 2e). As the NAOI shifts to neutral, the jet returns toward its climatological tilt and meridional location.

The PNAI initially oscillates around near-zero values, increasing to values of around +0.5 as the cold spells evolve (Figure 2e). At negative lags, the large geopotential height anomalies associated with the cold spells are misaligned with the PNA's poles. As the whole pattern shifts eastward, the anomalies are brought in close alignment with the PNA, resulting in a stronger projection (Figures 1g–1i). At larger positive lags the circulation over the North American continent shifts to a more zonal configuration, the negative temperature anomalies weaken, and the PNAI falls again to zero.

5. Discussion and Conclusions

The large-scale circulation associated with cold spells in eastern North America corresponds to advection of cold air from the Arctic region and to a very zonal and intense North Atlantic jet, shifted south of its climatological location. The largest anomalies in the large-scale flow are witnessed in the days around the peak of the cold spells (Figure S5). However, the zonalization of the flow across the North Atlantic is already evident 2 weeks prior to the peak of the cold spells and lasts uninterrupted for around 3 weeks (Figure 2a). This persistence is remarkable and is not an artifice of the smoothing applied to the anomalies (see Figure S9); as a term of comparison, *Franzke et al.* [2011a] identified three preferred jet regimes using the JLI and found that the jet rarely spends more than 2 weeks in the southern location.

To test the sensitivity of our results to the choice of domain used to identify the North American cold spells, we repeated the analysis using northward and southward shifted domains (Figures S2 and S3). If the domain used to identify the cold spells is shifted northward, the anomalous circulation discussed in section 3 follows this shift and is generally weakened; on the other hand, a southward-shifted domain does not correspond to weakened anomalies (Figure S3). This is potentially linked to the influence the choice of domain has on the jet entry location. When the cold air advection associated with the cold spells extends into the subtropical climate zone, it provides a highly baroclinic environment by enhancing the land-sea contrast on the eastern seaboard of North America; if this region is shifted North, it is natural to expect that the preference for a southern, intensified zonal jet and an increased storminess over western Europe will be weakened. Nonetheless, in both cases the southward displacement, zonalization, and intensification of the jet during the selected cold spells are conducive to the occurrence of destructive windstorms and intense precipitation over large parts of continental and southern Europe and the British Isles, as discussed in sections 3 and 4.

Based on these considerations, one might expect a bi-directional statistical link between the cold spells and the windstorms. In section 3 it was shown that by identifying the most severe cold spells over North America, one may recover destructive surface wind episodes over Europe. Similarly, by selecting the most destructive surface wind episodes over western Europe one indeed recovers below-average temperatures over North America (see Text S10). However, there is no one-to-one correspondence between the two sets of events, suggesting that extreme North American cold spells are neither a necessary nor a sufficient condition for the occurrence of heightened wind destructiveness over Europe. Rather, we interpret them as a statistically significant and physically plausible precursor.

The Atlantic circulation anomalies project onto the negative NAO at negative time lags, and there is a close correspondence between the JAI and JLI and the NAOI throughout the evolution of the spells. Indeed, *Woollings et al.* [2008, 2010a, 2010b] have suggested the existence of a negative NAO regime corresponding to a southern jet location and high-latitude blocking over Greenland; moreover, *Hurrell* [1995] found an enhanced moisture transport toward continental Europe during negative NAO events, and *Trigo et al.* [2004] found positive precipitation anomalies over Iberia. However, it would be incorrect to interpret the large-scale anomalies described in section 3 as a subset of the conditions associated with the negative phase of the NAO. Indeed, roughly one quarter of the cold spells displays positive NAOI values at small negative lags. Moreover, *Messori and Caballero* [2015] have shown that the jet's tilt exhibits a large variability unrelated to the NAOI, and negative NAO phases typically correspond to a weaker, less eastward extended jet [cf. *Pinto and Raible*, 2012], opposite to what is found for the selected cold spells. Finally, negative NAO events considered as a whole correspond to a statistically significant decrease in destructiveness across the analysis domain (Table 1).

The PNA shows a preference for the positive phase during the cold spells, peaking at small positive lags. This is consistent with previous work [*Cellitti et al.*, 2006] showing the onset and development of cold air outbreaks over North America to be associated with increasingly positive PNAI values (cf. Figure 2e with Figure 10 in *Cellitti et al.* [2006], noting that their day 0 corresponds to the onset and not the peak of the cold spell). However, the PNA pattern has previously been associated with positive temperature anomalies over western Canada and USA, as opposed to the continent-wide negative anomalies found here (*cf.* Figure 1 with Figure 2 in *Leathers et al.* [1991]). In fact, the geopotential anomaly dipole over the North Pacific associated with the cold spells resembles more closely the West Pacific Pattern [*Linkin and Nigam*, 2008], which has been previously linked with cold temperatures over large portions of North America [e.g., *Rogers*, 1981; *Hsu and Wallace*, 1985; *Linkin and Nigam*, 2008; *Lee et al.*, 2015]. Moreover, neither phase of the PNA has any significant impact on wind destructiveness over Europe (Table 1). Additional modes of climate variability, such as El-Niño/Southern Oscillation, have been associated with both below-average temperatures over the eastern United States [e.g., *Ropelewski and Halpert*, 1986] and increased storminess over Europe [e.g., *Fraedrich and Müller*, 1992] and may provide scope for future investigations.

As others before us [e.g., *Loikith and Broccoli*, 2014; *Grotjahn et al.*, 2015], we therefore interpret the circulation anomalies associated with extreme North American cold spells as being distinct from these canonical modes of climate variability. The wave activity flux displayed in Figures 1g–1i and S11 indeed suggests that the drivers of the anomalous cold spell circulation might be different from those associated with the climate modes. During the days prior to the North American temperature minima (Figures 1g and S11a and S11b), a wave train can be seen emanating from the subtropical central Pacific, arching over North America and turning north toward Greenland, tying together the Pacific, North American, and Atlantic circulation anomalies discussed earlier into a single hemispheric pattern [*Drouard et al.*, 2015]. At around lag 0, however, as the cyclonic anomaly over eastern North America reaches its maximum amplitude, the wave activity flux emanating from it turns south and enters the western subtropical Atlantic, generating an anticyclonic anomaly there and leading to the changeover from negative to neutral NAO conditions (Figure 1h). These results point to a possible major role for hemispheric-scale teleconnections in coordinating extreme events across North America and Europe, which provides a promising avenue for future work on prediction and prevention of climate-related impacts.

Acknowledgments
ERA-Interim reanalysis data are freely available from the ECMWF at http://apps.ecmwf.int/datasets/. G. Messori has been funded by the Swedish Vetenskapsrådet, as part of the MILEX project. We are grateful to T.J. Woollings and B.J. Hoskins for their helpful discussions. We also thank the two anonymous reviewers whose comments have helped to strengthen our conclusions.

References

Barnes, E. A., and J. A. Screen (2015), The impact of Arctic warming on the midlatitude jet-stream: Can it? Has it? Will it? *WIREs Clim. Change*, *6*, 277–286.

Cellitti, M. P., J. E. Walsh, R. M. Rauber, and D. H. Portis (2006), Extreme cold air outbreaks over the United States, the polar vortex, and the large-scale circulation, *J. Geophys. Res.*, *111*, D02114, doi:10.1029/2005JD006273.

Christidis, N., and P. A. Stott (2015), Extreme rainfall in the United Kingdom during winter 2013/2014: The role of atmospheric circulation and climate change [in "Explaining Extremes of 2014 from a Climate Perspective"], *Bull. Am. Meteorol. Soc.*, *96*(12).

Coumou, D., and S. Rahmstorf (2012), A decade of weather extremes, *Nat. Clim. Change*, *2*, 491–496.

Dee, D. P., et al. (2011), The ERA-Interim reanalysis: Configuration and performance of the data assimilation system, *Q. J. R. Meteorol. Soc.*, *137*(656), 553–597.

Drouard, M., G. Rivière, and P. Arbogast (2015), The link between the North Pacific climate variability and the North Atlantic Oscillation via downstream propagation of synoptic waves, *J. Clim.*, *28*, 3957–3976.

Fink, A. H., T. Brücher, V. Ermert, A. Krüger, and J. G. Pinto (2009), The European storm Kyrill in January 2007: Synoptic evolution, meteorological impacts and some considerations with respect to climate change, *Nat. Hazards Earth Syst. Sci.*, *9*, 405–423, doi:10.5194/nhess-9-405-2009.

Fraedrich, K., and K. Müller (1992), Climate anomalies in Europe associated with ENSO extremes, *Int. J. Climatol.*, *12*(1), 25–31.

Francis, J., and N. Skific (2015), Evidence linking rapid Arctic warming to mid-latitude weather patterns, *Phil. Trans. R. Soc. A*, *373*, 20140170, doi:10.1098/rsta.2014.0170.

Franzke, C., T. Woollings, and O. Martius (2011a), Persistent circulation regimes and preferred regime transitions in the North Atlantic, *J. Atmos. Sci.*, *68*(12), 2809–2825.

Gaetani, M., M. Baldi, G. A. Dalu, and G. Maracchi (2011), Jetstream and rainfall distribution in the Mediterranean region, *Nat. Hazards Earth Syst. Sci.*, *11*, 2469–2481, doi:10.5194/nhess-11-2469-2011.

Gómara, I., J. G. Pinto, T. Woollings, G. Masato, P. Zurita-Gotor, and B. Rodríguez-Fonseca (2014a), Rossby wave-breaking analysis of explosive cyclones in the Euro-Atlantic sector, *Q. J. R. Meteorol. Soc.*, *140*(680), 738–753.

Gómara, I., B. Rodríguez-Fonseca, P. Zurita-Gotor, and J. G. Pinto (2014b), On the relation between explosive cyclones affecting Europe and the North Atlantic Oscillation, *Geophys. Res. Lett.*, *41*, 2182–2190, doi:10.1002/2014GL059647.

Grotjahn, R., et al. (2015), North American extreme temperature events and related large scale meteorological patterns: A review of statistical methods, dynamics, modeling, and trends, *Clim. Dyn.*, 1–34.

Gu, L., P. Hanson, W. Post, D. Kaiser, B. Yang, R. Nemani, S. Pallardy, and T. Meyers (2008), The 2007 eastern US spring freezes: Increased cold damage in a warming world?, *BioScience*, *58*, 253–262.

Guirguis, K., A. Gershunov, R. Schwartz, and S. Bennett (2011), Recent warm and cold daily winter temperature extremes in the Northern Hemisphere, *Geophys. Res. Lett.*, *38* L17701, doi:10.1029/2011GL048762.

Hanley, J., and R. Caballero (2012), The role of large-scale atmospheric flow and Rossby wave breaking in the evolution of extreme windstorms over Europe, *Geophys. Res. Lett.*, *39*, L21708, doi:10.1029/2012GL053408.

Hsu, H.-H., and J. M. Wallace (1985), Vertical structure of wintertime teleconnection patterns, *J. Atmos. Sci.*, *42*, 1693–1710.
Huntingford, C., T. Marsh, A. A. Scaife, E. J. Kendon, J. Hannaford, A. L. Kay, and M. R. Allen (2014), Potential influences on the United Kingdom's floods of winter 2013/2014, *Nat. Clim. Change*, *4*(9), 769–777.
Hurrell, J. W. (1995), Decadal trends in the North Atlantic Oscillation: Regional temperatures and precipitation, *Science*, *269*(5224), 676–679.
Kendon, M., and M. McCarthy (2015), The UK's wet and stormy winter of 2013/2014, *Weather*, *70*(2), 40–47.
Klawa, M., and U. Ulbrich (2003), A model for the estimation of storm losses and the identification of severe winter storms in Germany, *Nat. Hazards Earth Syst. Sci.*, *3*, 725–732.
Konrad, C. E., II, and S. J. Colucci (1989), An examination of extreme cold air outbreaks over Eastern North America, *Mon. Weather Rev.*, *117*, 2687–2700, doi:10.1175/1520-0493(1989)117<2687:AEOECA>2.0.CO;2.
Kutiel, H., P. Maheras, and S. Guika (1996), Circulation and extreme rainfall conditions in the eastern Mediterranean during the last century, *Int. J. Climatol.*, *16*, 73–92.
Leathers, D. J., B. Yarnal, and M. A. Palecki (1991), The Pacific/North American teleconnection pattern and United States climate. Part I: Regional temperature and precipitation associations, *J. Clim.*, *4*(5), 517–528.
Lee, M. Y., C. C. Hong, and H. H. Hsu (2015), Compounding effects of warm sea surface temperature and reduced sea ice on the extreme circulation over the extratropical North Pacific and North America during the 2013–2014 boreal winter, *Geophys. Res. Lett.*, *42*, 1612–1618, doi:10.1002/2014GL062956.
Linkin, M. E., and S. Nigam (2008), The North Pacific Oscillation-West Pacific Teleconnection Pattern: Mature-phase structure and winter impacts, *J. Clim.*, *21*, 1979–1997, doi:10.1175/2007JCLI2048.1.
Liu, J., J. Curry, and H. Wang (2012), Impact of declining Arctic sea ice on winter snowfall, *Proc. Natl. Acad. Sci. U.S.A.*, *109*(11), 4074–4079, doi:10.1073/pnas.1114910109.
Loikith, P. C., and A. J. Broccoli (2012), Characteristics of observed atmospheric circulation patterns associated with temperature extremes over North America, *J. Clim.*, *25*(20), 7266–7281.
Loikith, P. C., and A. J. Broccoli (2014), The influence of recurrent modes of climate variability on the occurrence of winter and summer extreme temperatures over North America, *J. Clim.*, *27*(4), 1600–1618.
Maheras, P., E. Xoplaki, T. Davies, J. Martin-Vide, M. Bariendos, and M. J. Alcoforado (1999), Warm and cold monthly anomalies across the Mediterranean basin and their relationship with circulation; 1860–1990, *Int. J. Climatol.*, *19*(15), 1697–1715.
Matthews, T., C. Murphy, R. L. Wilby, and S. Harrigan (2014), Stormiest winter on record for Ireland and UK, *Nat. Clim. Change*, *4*(9), 738–740.
Messori, G., and R. Caballero (2015), On double Rossby wave breaking in the North Atlantic, *J. Geophys. Res. Atmos.*, *120*, 11,129–11,150, doi:10.1002/2015JD023854.
Palmer, T. (2014), Record-breaking winters and global climate change, *Science*, *344*(6186), 803–804.
Pinto, J. G., and C. C. Raible (2012), Past and recent changes in the North Atlantic oscillation, *Wiley Interdiscip. Rev. Clim. Change*, *3*(1), 79–90.
Pinto, J. G., I. Gómara, G. Masato, H. F. Dacre, T. Woollings, and R. Caballero (2014), Large-scale dynamics associated with clustering of extratropical cyclones affecting western Europe, *J. Geophys. Res. Atmos.*, *119*, 13,704–13,719, doi:10.1002/2014JD022305.
Poli, P., et al. (2016), ERA-20C: An atmospheric reanalysis of the 20th century, *J. Clim.*, doi:10.1175/JCLI-D-15-0556.1.
Portis, D. H., M. P. Cellitti, W. L. Chapman, and J. E. Walsh (2006), Low-frequency variability and evolution of North American cold air outbreaks, *Mon. Weather Rev.*, *134*(2), 579–597.
Raveh-Rubin, S., and H. Wernli (2015), Large-scale wind and precipitation extremes in the Mediterranean: A climatological analysis for 1979–2012, *Q. J. R. Meteorol. Soc.*, *141*, 2404–2417, doi:10.1002/qj.2531.
Rivière, G., and A. Joly (2006), Role of the low-frequency deformation field on the explosive growth of extratropical cyclones at the jet exit. Part II: Baroclinic critical region, *J. Atmos. Sci.*, *63*, 1982–1995.
Rogers, J. C. (1981), The North Pacific Oscillation, *J. Climatol.*, *1*, 39–57.
Ropelewski, C. F., and M. S. Halpert (1986), North American precipitation and temperature patterns associated with the El Niño/Southern Oscillation (ENSO), *Mon. Weather Rev.*, *114*(12), 2352–2362.
Santos, J. A., T. Woollings, and J. G. Pinto (2013), Are the winters 2010 and 2012 archetypes exhibiting extreme opposite behavior of the North Atlantic jet stream?, *Mon. Weather Rev.*, *141*, 3626–3640.
Screen, J. A., and I. Simmonds (2014), Amplified mid-latitude planetary waves favour particular regional weather extremes, *Nat. Clim. Change*, doi:10.1038/nclimate2271.
Slingo, J., et al. (2014), The recent storms and floods in the UK. Met Office, Exeter, U. K. [Available at http://www.metoffice.gov.uk/media/pdf/1/2/Recent_Storms_Briefing_Final_SLR_20140211.pdf.]
Takaya, K., and H. Nakamura (2001), A formulation of a phase-independent wave-activity flux for stationary and migratory quasigeostrophic eddies on a zonally varying basic flow, *J. Atmos. Sci.*, *58*(6), 608–627.
Trenary, L., T. DelSole, M. K. Tippett, and B. Dotty (2015), Was the cold eastern US winter of 2014 due tro Increased Variability?, [in "Explaining Extremes of 2014 from a Climate Perspective"], *Bull. Am. Meteorol. Soc.*, *96*(12).
Trigo, R. M., D. Pozo-Vázquez, T. J. Osborn, Y. Castro-Díez, S. Gámiz-Fortis, and M. J. Esteban-Parra (2004), North Atlantic oscillation influence on precipitation, river flow and water resources in the Iberian Peninsula, *Int. J. Climatol.*, *24*, 925–944, doi:10.1002/joc.1048.
van Oldenborgh, G. J., D. B. Stephenson, A. Sterl, R. Vautard, P. Yiou, S. S. Drijfhout, H. van Storch, and H. van den Dool (2015), Drivers of the 2013/2014 winter floods in the UK, *Nat. Clim. Change*, *5*(6), 490–491.
Wallace, J. M., and D. S. Gutzler (1981), Teleconnections in the geopotential height field during the Northern Hemisphere winter, *Mon. Weather Rev.*, *109*, 784–812.
Walsh, J. E., A. S. Phillips, D. H. Portis, and W. L. Chapman (2001), Extreme cold outbreaks in the United States and Europe, 1948–1999, *J. Clim.*, *14*(12), 2642–2658.
Wang, C., H. Liu, and S. K. Lee (2010), The record-breaking cold temperatures during the winter of 2009/2010 in the Northern Hemisphere, *Atmos. Sci. Lett.*, *11*(3), 161–168.
Wild, S., D. J. Befort, and G. C. Leckebush (2015), Was the extreme storm season in winter 2013/2014 over the North Atlantic and the United Kingdom triggered by changes in the west Pacific warm pool?, [in "Explaining Extremes of 2014 from a Climate Perspective"], *Bull. Am. Meteorol. Soc.*, *96*(12).
Woollings, T. J., B. J. Hoskins, M. Blackburn, and P. Berrisford (2008), A new Rossby wave-breaking interpretation of the North Atlantic Oscillation, *J. Atmos. Sci.*, *65*, 609–626.
Woollings, T. J., A. Hannachi, B. J. Hoskins, and A. Turner (2010b), A regime view of the North Atlantic Oscillation and its response to anthropogenic forcing, *J. Clim.*, *23*, 1291–1307.

Woollings, T., A. Hannachi, and B. J. Hoskins (2010a), Variability of the North Atlantic eddy-driven jet stream, *Q. J. R. Meteorol. Soc.*, *136*, 856–868, doi:10.1002/qj.625.

Yu, Y., M. Cai, R. Ren, and H. M. van den Dool (2015a), Relationship between warm air mass transport into the upper polar atmosphere and cold air outbreaks in winter, *J. Atmos. Sci.*, *72*(1), 349–368.

Yu, Y., R. Ren, and M. Cai (2015b), Comparison of the mass circulation and AO indices as indicators of cold air outbreaks in northern winter, *Geophys. Res. Lett.*, *42*, 2442–2448, doi:10.1002/2015GL063676.